

Terpyridineplatinum(II) Incorporation in *N*-Methylpyrrole-Based Polyamides by Solid Phase Techniques

Marcelis van Holst,^[a] Delphine Le Pevelen,^[b] and Janice Aldrich-Wright^[a]

Dedicated to Professor Jan Reedijk on the occasion of his retirement

Keywords: Polyamides / Anticancer agents / Platinum / Terpyridine / Solid phase synthesis

The incorporation of terpyridineplatinum(II) centres into sequence-selective polyamides has been explored in this study, with the aim of producing cytotoxic molecules that display DNA sequence specificity. To facilitate this a terpyridineplatinum(II)-based metallointercalator has been developed, which can be incorporated into sequence-selective polyamides using standard machine-assisted peptide coupling

techniques. A novel *N*-methylpyrrole-based metallopolyamide, containing the new terpyridineplatinum(II) moiety, was also synthesised to validate this new method of incorporation.

(© Wiley-VCH Verlag GmbH & Co. KGaA, 69451 Weinheim, Germany, 2008)

Introduction

Cancer is a leading cause of illness and death in developed countries. Current anticancer drugs are limited by side-effects and the ability of malignant cells to become resistant to treatment.^[1–3] New drugs that display the potential to target cancerous cells, without affecting healthy cells, are of great interest.^[4–12] This may be achieved by designing novel molecules that bind to specific targets that are exclusive to, or are highly conserved within, cancer cells. Some naturally occurring groove-binding polyamides, such as netropsin and distamycin (Figure 1), display inherent specificity for DNA base pair sequences.^[13,14] Both structures comprise a series of heterocyclic rings linked by single bonds that can rotate to match the conformation of the target DNA site. Considerable efforts have been made to characterise the affinity of these heterocycles to specific base pairs, which has given rise to a set of base pairing rules that relate to the *anti*-parallel association of *N*-methylimidazole (Im), *N*-methylpyrrole (Py) and 3-hydroxy-*N*-methylpyrrole (Hp) containing polyamides to their predicted target DNA sequences.^[15–17]

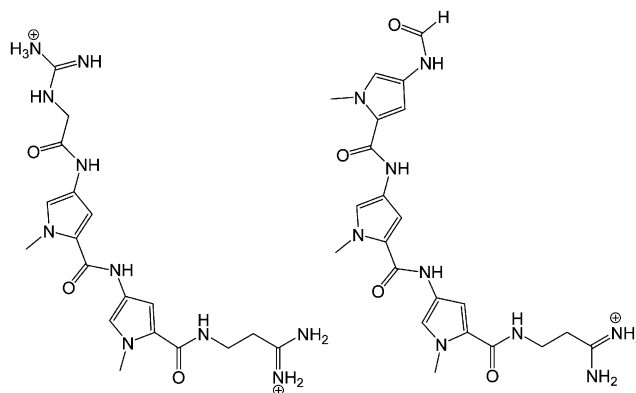


Figure 1. The structures of netropsin (left) and distamycin (right).

This facilitates the selection of specific groups in the polyamide chain on the basis of the nucleotide sequence of interest. Heterocyclic rings can be selected from a pool consisting of Im, Py and Hp, which form four ring-pairings (Im/Py, Py/Im, Hp/Py, Py/Hp) that can distinguish between all four Watson–Crick base pairs.^[18] Additionally, a Py/Py ring-pairing binds to both T:A and A:T sequences but cannot distinguish between them. The binding preferences of each heterocyclic pairing is governed by hydrogen-bonding and steric effects between the ligand and specific hydrogen-bond donors and acceptors on the floor of the minor groove.^[19–23]

Due to their unique binding characteristics, sequence-selective polyamides have been under investigation as potential anticancer agents for some time. The incorporation of platinum(II) centres into such molecules has been investi-

[a] School of Biomedical and Health Sciences, University of Western Sydney, Locked Bag 1797, Penrith South DC, NSW, 1797, Australia
Fax: +61-4620-3025
E-mail: j.aldrich-wright@uws.edu.au

[b] Chiralabs Ltd, BCIE, Oxford University Begbroke Science Park, Sandy Lane, Yarnton, Oxfordshire, OX5 1PF, UK
E-mail: d.lepevelen@chiralabs.com

Supporting information for this article is available on the WWW under <http://www.eurjic.org> or from the author.

gated as a means of increasing their cytotoxicity. Distamycin has been conjugated with cisplatin to form the two isomers Pt-DIST(R) and Pt-DIST(S).^[24,25] Whilst the DNA binding mode of these complexes was different to cisplatin, with an increase in interstrand cross-links observed, the selectivity of the platinum(II) complex for GG and AG sequences was not significantly altered by the polyamide component.^[24,25] Further research has focused on achieving greater synergy between the two structural motifs. Recently the synthesis of the transplatin-based molecules DJ1953-2 and DJ1953-6, which contain a sequence-selective polyamide component designed to recognise the DNA sequence 5'-TG(T/A)CA-3' (Figure 2), was reported.^[26]

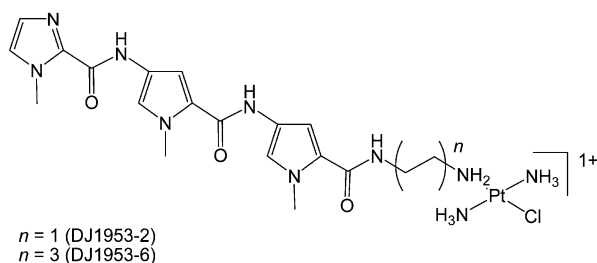


Figure 2. The general structure of compounds in the DJ1953 family of platinum(II) complexes.

Whilst neither metal complex displayed significant cytotoxicity, they were more active than distamycin and netropsin. The synthetic schemes for DJ1953-2 and DJ1953-6 were both challenging and low yielding. To address this, new methods were devised whereby transplatin complexes with

either linear or hairpin polyamide ligands were assembled entirely by Fmoc-based solid phase techniques.^[27] This process involves the step-wise formation of the product on an inert support, from which it is later cleaved under mild conditions. The ease of purification afforded by the inert support allows excess reagents to be used, which greatly increases the efficiency of the reactions. Unfortunately the products of these reactions, HLSP-6 and HLWC-8 (Figure 3), have poor water solubility.^[27]

Alternative platinum(II) DNA binding moieties are now being explored, with the aim of further characterising the structure/activity relationships of this family of molecules. In this study a new terpyridineplatinum(II)-based metallointercalator, [Pt(terpy)(mpa)]PF₆ (**1**), was developed for incorporation into sequence-selective polyamides using standard, organic-based, machine-assisted peptide coupling techniques (Figure 4).

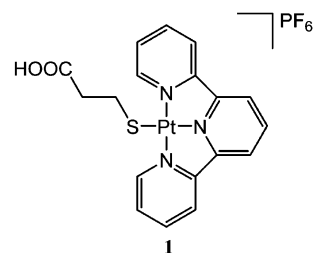


Figure 4. [Pt(terpy)(mpa)]PF₆ (**1**).

This molecule was then used in the solid phase assembly of an *N*-methylpyrrole-based metallopolyamide.

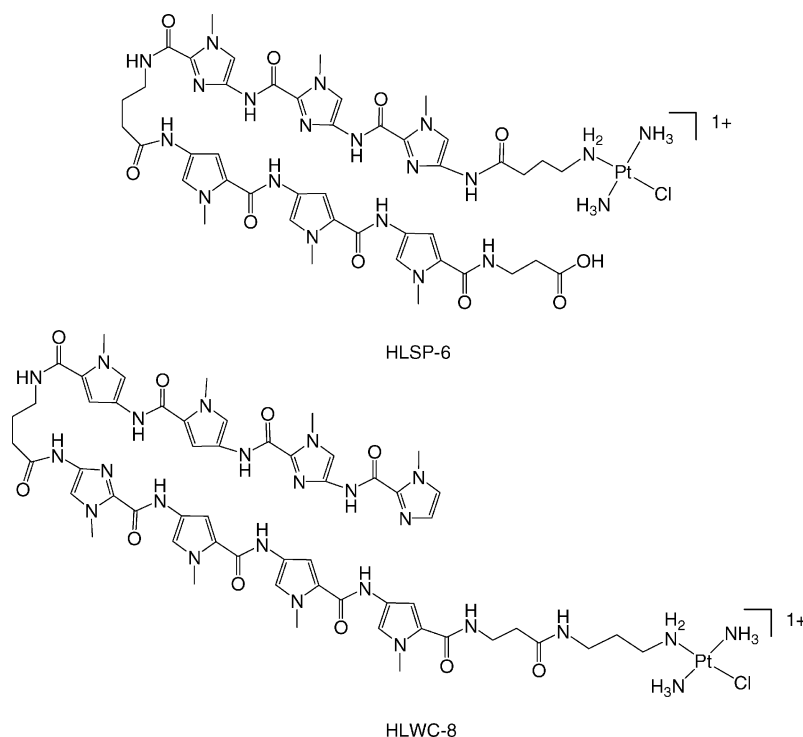


Figure 3. The transplatin-based polyamides HLSP-6 and HLWC-8, which have been synthesised using solid phase methods.^[27]

Results and Discussion

Metal Complex Synthesis

Compound **1** was obtained by the reaction of commercially available 3-mercaptopropanoic acid with [Pt(terpy)-Cl]Cl, which was synthesised in a two-step process following the methods of McDermott and Annibale.^[28,29]

[Pt(terpy)Cl]Cl was dissolved in a small amount of H₂O through which a continuous stream of nitrogen was bubbled. Three equivalents of the base tetrabutylammonium hydroxide were added to this solution, followed by one equivalent of 3-mercaptopropionic acid, causing an immediate colour change from orange to dark purple. It should be noted that if the ligand is added before the base, the reaction does not work. The product was isolated as quickly as possible by concentration under vacuum and precipitation by the addition of acetone. The fine purple solid was collected by vacuum filtration, then immediately redissolved in H₂O and precipitated by the addition of a saturated PF₆ solution. The crude product was then purified by a series of salt conversions from PF₆ to Br and back to PF₆, using a saturated PF₆ solution and tetrabutylammonium bromide in ACN. Initial attempts to synthesise **1** utilised silver nitrate to activate the [Pt(terpy)Cl]Cl species prior to coordination. This provided no increase in the yield and silver chloride contamination was problematic.

NMR Characterisation

The product, **1**, was characterised by one and two-dimensional ¹H NMR spectroscopy. The ¹H resonances for **3** moved upfield as a function of increasing concentration, suggesting strong intermolecular stacking interactions. This is consistent with previously published observations for similar terpyrideneplatinum(II) complexes.^[30] The 6-H resonances displayed the greatest shift under these conditions, moving twice as far as the other aromatic resonances.

The doublet furthest downfield in the spectrum of **1** displays platinum coupling and is assigned as 6-H. This resonance appears 0.8–1.7 ppm further upfield in the equivalent spectrum of [Pt(terpy)Cl]Cl, and is a clear indicator of ligand coordination. Proton 6-H is coupled to 5-H (*J*_{5-H-6-H} = 6.2 Hz). The triplet at ca. 7.55 ppm integrating for two protons corresponds to the 5-H proton. The complex multiplet at ca. 8.15 ppm was assigned as the 4-H and 4'-H resonances, whilst the complex multiplet at ca. 8.05 ppm was assigned as the 3-H and 3'-H resonances, integrating to 3 and 4 protons respectively. Interestingly, the 7-H and 8-H protons of **3** appear at the same chemical shift in D₂O, as a singlet integrating for 4 protons. These peaks are slightly better resolved in organic solvents, such as [D₃]-ACN and [D₇]-DMF. The acidic proton labelled 9-H is only visible in ¹H spectra obtained using organic solvents with non-exchangeable protons and was assigned as the resonance at δ = 12.04 ppm. The proton assignments are displayed in Figure 5.

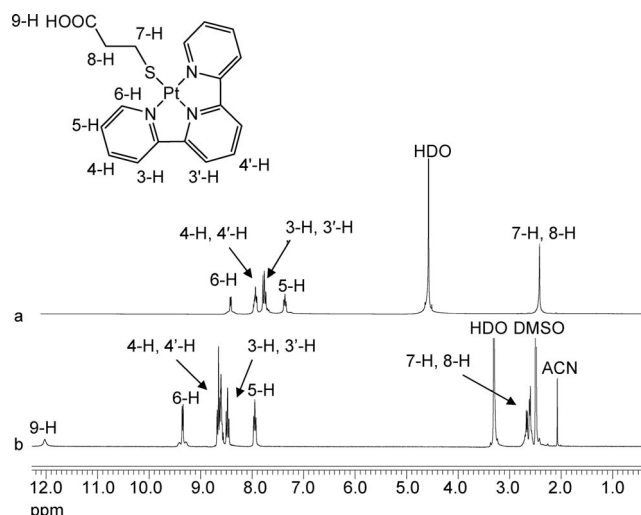


Figure 5. The proton numbering scheme, ¹H NMR spectra in D₂O (a) and [D₇]DMSO (b) and proton assignments of compound **1**.

The ¹⁹⁵Pt spectrum of **1** displays a single peak at –3211.71 ppm; an upfield shift of 490.57 ppm when compared to [Pt(terpy)Cl]Cl. This was indicative of the replacement of a chloride ligand for sulfur in the platinum coordination sphere.

X-ray Crystal Structure

The tendency of platinum terpyridine complexes to aggregate in solution has been studied previously, and is usually governed by strong π - π interactions.^[30] Of those studies, the X-ray crystal structure of [Pt(terpy)(HET)]NO₃^[30] was of special interest. The orientation of the mercaptoethanol tail was expected to influence the packing arrangement due to hydrogen bonding, in a similar manner to the carboxylic acid component of **1**. Such interactions would be expected to have an effect on the DNA binding properties of the molecules. Attempts to grow crystals of pure compound **1** for analysis by single crystal X-ray diffraction were unsuccessful. Suitable crystals were obtained serendipitously, from the product of an earlier reaction that utilised AgNO₃ to activate the [Pt(terpy)Cl]Cl species. The structure of the complex is well resolved, revealing an asymmetric unit consisting of two equivalent [Pt(terpy)(mpa)]⁺ complexes, one silver chloride molecule, one chloride counterion and five water molecules which are disordered (Figure 6).

The coordination geometry of [Pt(terpy)(mpa)]⁺ is essentially square planar with distortion caused by the steric constraints imparted by the tridentate terpyridine ligand. The H atoms were all located in a difference map, but those attached to carbon atoms were repositioned geometrically. The H atoms were initially refined with soft restraints on the bond lengths and angles to regularise their geometry (C–H in the range 0.93–0.98 Å, N–H in the range 0.86–0.89 Å and O–H = 0.82 Å) after which the positions were refined with riding constraints. The chloride counterions, which are required to balance the 1+ charge of the metal

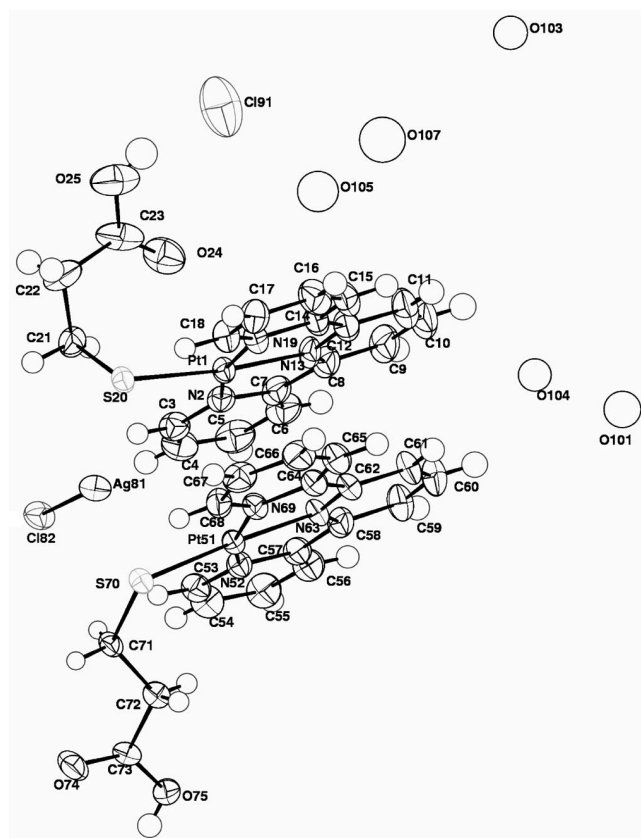


Figure 6. The ORTEP diagram of the species $[\text{Pt}(\text{terpy})(\text{mpa})]^+$ displaying the atom numbering scheme. Hydrogen atoms are not numbered. Free oxygen atoms (numbered O101, O103, O104, O105 and O107) belong to water molecules.

complex, were not well described in the crystal structure. It was first hypothesised that some of the carboxylic acid groups may be ionising to provide the balance in charge, but closer observation of the differential bond lengths suggests that only neutral carboxylic acid groups are present. Furthermore, the presence of a small electron density indicated the presence of a hydrogen atom on each of those groups. Possible explanations for this anomaly include the counterion existing in a channel of disordered density in the centre of the crystal packing columns, random ionisation of the carboxylic acid groups or an unexpected charge state of the metal complex.

For each $[\text{Pt}(\text{terpy})(\text{mpa})]^+$ unit in the crystal structure, the Pt–N distance to the middle nitrogen atom of the terpyridine ligand [N13 and N63; 1.969(4) Å] is slightly shorter than the distances of each platinum to the other nitrogen atoms in the coordinated ligand [N2 and N19; 2.029(4) Å and 2.026(5) Å respectively, as well as N52 and N69; 2.047(4) Å and 2.032(4) Å respectively]. This characteristic is highly conserved amongst terpyridineplatinum(II) complexes. The mercaptoethanol analogue $[\text{Pt}(\text{terpy})(\text{HET})]\text{NO}_3$ displays almost identical bond lengths in this regard, where the equivalent bond is 1.968(5) Å [slightly shorter than the other Pt–N bonds; 2.023(5) Å and 2.030(5) Å respectively].^[30] Other complexes in this family such as

$[\text{Pt}(\text{terpy})(\text{NS})]\text{ClO}_4$ and the di-nuclear species $[\{\text{Pt}(\text{terpy})\}_2(\text{SNS})](\text{ClO}_4)_2$ also display Pt–N bond lengths that reflect this trend.^[31]

The N–Pt–N angles – 81.02(19)°, 80.50(19)°, 80.11(18)° and 80.69(18)° – are significantly smaller than the theoretical value of 90° expected for square-planar complexes. This is also characteristic of four coordinate terpyridineplatinum(II) complexes.^[30–33] The length of the bonds between platinum and sulfur; 2.2963(11) Å and 2.3064(11) Å, are comparable to the Pt–S distance of the complex $[\text{Pt}(\text{terpy})(\text{HET})]\text{NO}_3$ which has a Pt–S distance of 2.303(2) Å.^[30,31] The N–Pt–S angles – 102.74(13)°, 95.86(12)°, 106.82(12)° and 92.49(12)° – further reflect the strain caused by chelation of the terpyridine ligand and is comparable with complexes of similar structure. The mercapto ligand of the $[\text{Pt}(\text{terpy})(\text{mpa})]^+$ species has less conformational freedom due to the interaction with the Ag atom of AgCl [2.4552(13) Å and 2.4685(13) Å], unlike the crystal structure of $[\text{Pt}(\text{terpy})(\text{HET})]\text{NO}_3$ which displayed disorder of the mercaptoethanol carbon atoms.^[30] A summary of the bond lengths and angles pertaining to the coordination geometry and mercaptopropionic acid ligands are provided in Table 1.

Table 1. Selected bond lengths (Å) and angles [°] of $[\text{Pt}(\text{terpy})(\text{mpa})]^+$.

Pt1–S20	2.2963(11)	C21–C22	1.499(9)
Pt1–N2	2.029(4)	C22–C23	1.547(11)
Pt1–N13	1.969(4)	O24–C23	1.201(10)
Pt1–N19	2.026(5)	O25–C23	1.301(9)
S20–Pt1–N2	102.74(13)	Pt1–S20–C21	109.7(2)
S20–Pt1–N13	173.52(15)	S20–C21–C22	114.5(5)
N2–Pt1–N13	81.02(19)	C21–C22–C23	112.8(5)
S20–Pt1–N19	95.86(12)	C22–C23–O25	113.2(8)
N2–Pt1–N19	161.40(18)	C22–C23–O24	123.6(6)
N13–Pt1–N19	80.50(19)	O25–C23–O24	123.2(8)
S20–C21	1.827(6)		

The stacking interaction of $[\text{Pt}(\text{terpy})(\text{mpa})]^+$ is different to that of structurally similar mononuclear complexes due to the interaction of the AgCl molecule. The stacking interaction of $[\text{Pt}(\text{terpy})(\text{mpa})]^+$ involves a head-to-head motif which is stabilised by the presence of the AgCl (Figure 7). This is similar to the conformation adopted by di-nuclear species such as $[\{\text{Pt}(\text{terpy})\}_2(\text{SNS})]\text{ClO}_4$. The propanoic acid moiety extends perpendicular to the plane of the aromatic rings, similar to the mercaptoethanol ligand of $[\text{Pt}(\text{terpy})(\text{HET})]\text{NO}_3$.^[30]

The unique stacking arrangement of $[\text{Pt}(\text{terpy})(\text{mpa})]^+$ in the presence of AgCl has an effect on the crystal packing arrangement, which produces columns of $[\text{Pt}(\text{terpy})(\text{mpa})]^+$ stabilised by silver ions (Figure 8). Distinct layers are observed containing the platinum centres, terpyridine ligands, sulfur atoms and AgCl molecules, with the propanoic acid moiety projecting between the layers. Between the columns are channels of disordered atoms, possible due to water molecules and/or counterions. In comparison, the complex $[\text{Pt}(\text{terpy})(\text{HET})]\text{NO}_3$ forms sheets within the crystal lattice stabilised by the previously described stacking interactions,

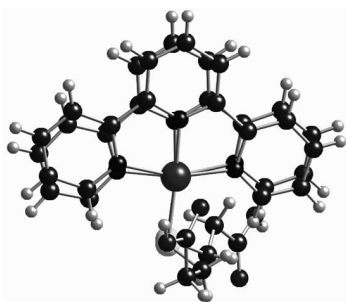


Figure 7. The stacking interaction of $[\text{Pt}(\text{terpy})(\text{mpa})]^+$ involving a head-to-head motif which is stabilised by the presence of AgCl .

with the cations laterally displaced from one unit cell to the next.^[30] This prevents the generation of a columnar stack perpendicular to the terpyridine plane.

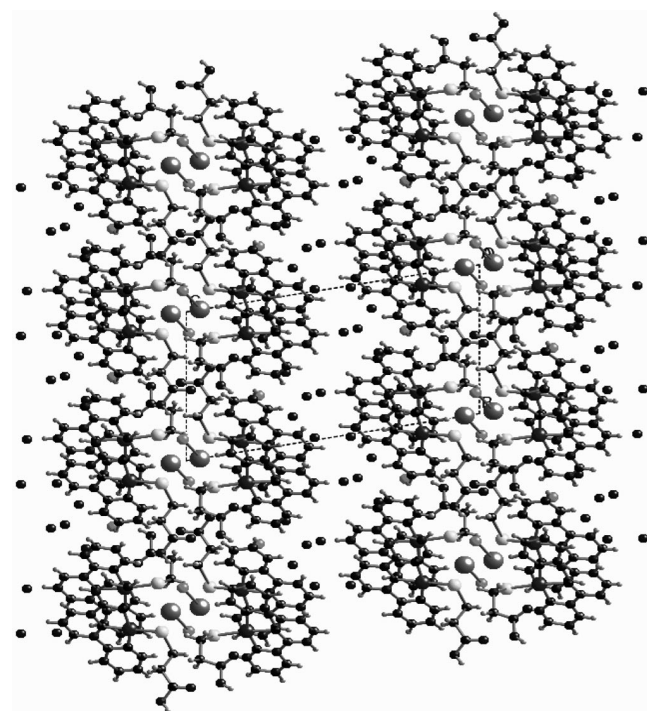


Figure 8. The crystal packing arrangement of $[\text{Pt}(\text{terpy})(\text{mpa})]^+$.

Metallopolyamide Synthesis

As a “proof of concept” $[\text{Pt}(\text{terpy})(\text{MPA})]\text{PF}_6$ was coupled to a sequence-selective polyamide comprising of three *N*-methylpyrrole and two β -alanine subunits by machine-assisted protocols.

The synthesis of the Fmoc-protected *N*-methylpyrrole monomer 4-[(9-fluorenylmethoxycarbonyl)amino]-*N*-methylpyrrole-2-carboxylic acid, in multigram quantities, has been reported previously.^[34–36]

Fmoc- β -ala-chlorotrityl resin was prepared by the Fmoc- β -alanine substitution of 2-chloro-chlorotrityl resin (0.44 mmol/g substitution level). The polyamide component

was elongated on solid phase from freshly prepared 4-[(9-fluorenylmethoxycarbonyl)amino]-*N*-methylpyrrole-2-carboxylic acid and commercially available Fmoc- β -alanine, with coupling cycles of approximately 210 min per residue (Figure 9).

A coupling cycle consists of several DCM and DMF washes to swell the resin, deprotection of the terminal Fmoc protecting group by treatment with 20% piperidine in DMF and manual addition of the next pre-activated subunit. This was followed by several DCM and DMF washing steps to remove any excess reagents in preparation for the next cycle. For the final addition step $[\text{Pt}(\text{terpy})(\text{mpa})]\text{PF}_6$ was dissolved in DMF and activated with HBTU and diisopropylethylamine (DIEA). The red solution was stirred for 5 min before it was added to the reaction vessel, followed by the resumption of automated synthesis. The final product was washed thoroughly with DMF and DCM whilst still on the solid support, until the reaction vessel consistently drained as a colourless solution. The resin was then washed manually with copious amounts of brine to convert the complex to a chloride salt. Cleavage of the final product was achieved using TFE and acetic acid, yielding a dark purple solution. The solvent was removed under reduced pressure and the product dried under vacuum and characterised by microanalysis. Whilst the resultant product displayed poor solubility, it proved the validity of the new synthetic procedure.

Conclusions

A new terpyridineplatinum(II) complex, $[\text{Pt}(\text{terpy})(\text{MPA})]\text{PF}_6$, has been synthesised specifically for the purposes of incorporation into sequence-specific polyamides by solid phase techniques. $[\text{Pt}(\text{terpy})(\text{MPA})]\text{PF}_6$ was successfully incorporated into a polyamide comprising of three *N*-methylpyrrole and two β -alanine subunits in 87% yield. Further investigations will focus on improving the solubility of metallopolyamides to facilitate DNA binding and biological activity assays. This may be achieved by the incorporation of heterocycles capable of hydrogen bonding (such as Im and Hp).

Experimental Section

Characterisation: ^1H NMR spectra were recorded on a 300 MHz Varian Unity *plus*. ^{195}Pt NMR spectra were obtained using a Bruker 400 Avance spectrometer (400 MHz). Commercially available deuterated solvents were used and referenced to the residual solvent H signal. Mass spectra were obtained at the Mass Spectrometry Laboratory at the University of Wollongong, NSW, Australia. Microanalysis was performed at the Australian National University, Canberra, ACT, Australia.

(3-Mercaptopropionic acid)terpyridineplatinum(II) Chloride $[\text{Pt}(\text{terpy})(\text{mpa})\text{Cl}]$ (1): $[\text{Pt}(\text{terpy})\text{Cl}]\text{Cl}\cdot 2\text{H}_2\text{O}$ (0.54 g, 1.0 mmol) was dissolved in H_2O (10 mL). A stream of $\text{N}_2(\text{g})$ was bubbled through the solution for the duration of the reaction. Three equivalents of tetrabutylammonium hydroxide was added (0.8 M in MeOH, 3.75 mL, 3.0 mmol). 3-Mercaptopropionic acid (0.27 g, 2.5 mmol)

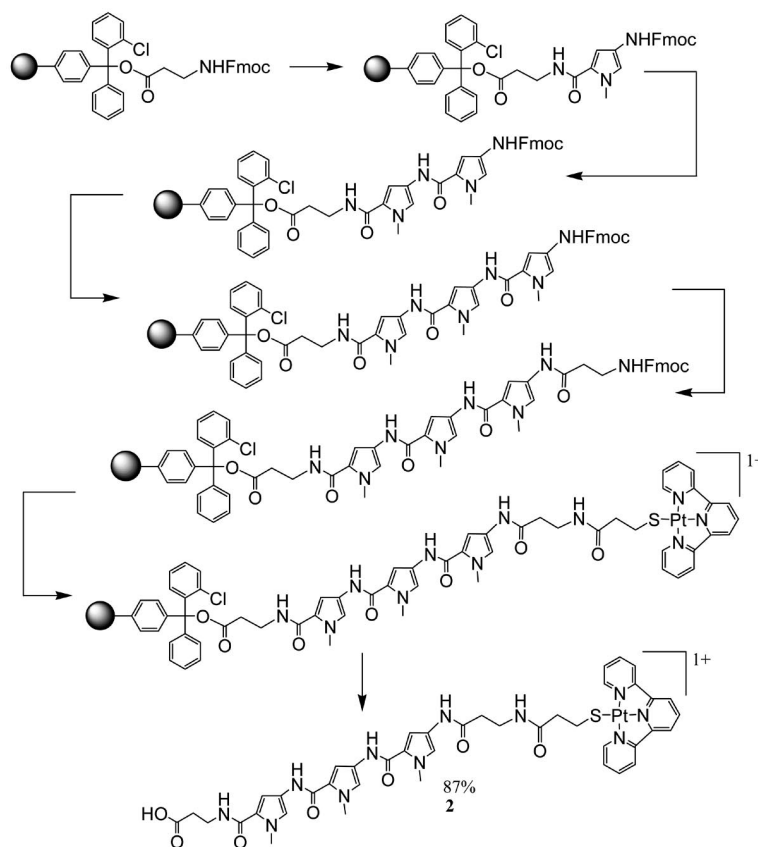


Figure 9. The reaction scheme for the synthesis of the terpyridineplatinum(II)-based polyamide **2**. Reaction conditions for each coupling cycle are provided in the experimental section.

was dissolved in H₂O (5 mL) and added to the basic solution of [Pt(terpy)Cl]Cl·2H₂O causing an instant colour change to purple. The solution was filtered (0.45 µm nylon membrane), reduced to ca. 5 mL under vacuum and dropped slowly into acetone (100 mL), resulting in the formation of a fine purple precipitate. The solid was collected by filtration through a 0.45 µm nylon filter, washed with acetone (50 mL), diethyl ether (50 mL) and air dried before being redissolved in a minimum amount of H₂O. The metal complex was precipitated by the addition of saturated KPF₆ solution (3 mL), the purple solid was collected, washed with diethyl ether (100 mL) and air dried. The complex was then dissolved in ACN (50 mL) before precipitation by the addition of a saturated tetrabutylammonium bromide/ACN solution. before being redissolved in a minimum amount of H₂O. The metal complex was precipitated by the addition of saturated KPF₆ solution (3 mL), the purple solid was collected, washed with diethyl ether (100 mL) and air dried (0.46 g, 81%). ¹H NMR (300 MHz, D₂O): δ = 8.6 (d, ¹J = 6.2 Hz, 2 H, 6-H), 8.11 (m, 3 H, 4-H and 4'-H), 7.93 (m, 4 H, 3-H and 3'-H), 7.51 (m, 2 H, 5-H), 2.42 (s, 4 H, 7-H and 8-H) ppm. ¹⁹⁵Pt NMR (85 MHz, D₂O): δ = -3211.71 (s) ppm. ESI-MS *m/z* calcd. for C₁₈H₁₆N₃O₂PtS [M + H]⁺ 533.48, found 533.2. C₁₈H₁₆F₆N₃O₂PS (483.37): calcd. C 31.86, H 2.38, N 6.19; found C 31.95, H 2.53, N 6.31.

Solid Phase Synthesis: Machine-assisted synthesis was performed on a Protein Technologies peptide synthesiser (model Symphony Quartet), using custom deprotection and coupling programs. Manual addition involved setting the solvent column as “none” within the program, setting the volume as “1 unit” (the program does not give the option of “0 units”), pausing the operation at the start of

the reaction step and manually pipetting the reagent into the reaction vessel.

Preparation of Fmoc-β-Ala-Chlorotrityl Resin: 2-Chloro-chlorotrityl resin (0.5 g, 0.5 mmol) was suspended in anhydrous DCM (5 mL). Separately, Fmoc-β-alanine (0.16 g, 0.5 mmol) in anhydrous DCM (4 mL) and DIEA (0.348 mL, 2 mmol) was stirred for 5 min. The Fmoc-β-Ala-COOH solution was added to the resin suspension and shaken for 5 h. Methanol (2.5 mL) was added and the mixture was shaken for 30 min. The resin was collected by filtration, washed with DCM and dried under vacuum overnight (0.56 g, 44% yield, 0.44 mmol/g loading).

Washing and Deprotection of Fmoc-β-Ala-Chlorotrityl Resin: Fmoc-β-ala-chlorotrityl resin was washed and prepared for coupling to the first pyrrole ring using the following step-wise program on a solid phase synthesiser (Table 2).

General Activation and Coupling Procedure: Fmoc-β-alanine or **8** (0.50 mmol) and HBTU (0.18 g, 0.48 mmol) were dissolved in DMF (5 mL). DIEA was added (0.26 mL, 1.5 mmol) and the mixture shaken for 5 min. The solution was added to the drained and deprotected resin by manual addition and mixed under nitrogen agitation for 3.5 h. The resin was drained in preparation for further elongation through deprotection of the new amino terminus.

General Deprotection Method: The substituted resin was washed and deprotected for coupling to the next subunit using the following stepwise program on a solid phase synthesiser (Table 3).

Activation and Coupling of [Pt(terpy)(MPA)]PF₆: [Pt(terpy)(MPA)]-PF₆ (0.34 g, 0.5 mmol) was dissolved in DMF (5 mL) as a PF₆ salt.

Table 2. The resin washing and deprotection program.

Step	Solvent	Volume (units) ^[a]	Time ^[b]	Drain	Repetitions
1	DCM	7	00:00:30	on	1
2	DMF	7	00:00:30	on	1
3	20% piperidine	7	00:03:00	on	1
4	20% piperidine	7	00:17:00	on	1
5	DMF	7	00:00:30	on	1
6	DCM	7	00:00:30	on	1
7	DMF	7	00:01:00	on	2

[a] The term "unit" is provided by the manufacturer of the solid phase apparatus, and equates to approximately 1.15 mL. [b] Time is given in the general form of HH:MM:SS.

Table 3. The program used for the deprotection of substituted resin.

Step	Solvent	Volume (units)	Time	Drain	Repetitions
1	DCM	7	00:00:30	on	1
2	DMF	7	00:00:30	on	1
3	20% piperidine	7	00:03:00	on	1
4	DMF	7	00:00:30	on	1
5	20% piperidine	7	00:03:00	on	1
6	DMF	7	00:00:30	on	1
7	DCM	7	00:00:30	on	1
8	DMF	7	00:01:00	on	2

HBTU (0.18 g, 0.48 mmol) and DIEA (0.26 mL, 1.5 mmol) were added and the mixture shaken for 5 min. The solution was added to the drained and deprotected resin by manual addition and mixed under nitrogen agitation for 5 h. The final compound was washed thoroughly on the resin using the regime outlined in Table 4.

Table 4. The final washing program for compound **10**, in preparation for resin cleavage.

Step	Solvent	Volume (units)	Time	Drain	Repetitions
1	DMF	7	00:00:30	yes	10
2	DCM	7	00:00:30	yes	5
3	brine ^[a]	7	00:03:00	yes	3
4	H ₂ O ^[a]	7	00:00:30	yes	5
5	DCM	7	00:03:00	yes	1
6	H ₂ O ^[a]	7	00:00:30	yes	5
7	DCM	7	00:00:30	yes	5

[a] Brine and H₂O were added by manual addition. In addition to this the H₂O was heated to between 50 °C and 60 °C prior to the addition, to aid in dissolving NaCl left over from the brine wash.

Cleavage of the Final Product (2): A solution of DCM (4.2 mL), trifluoroethanol (TFE, 1.2 mL) and acetic acid (0.6 mL) was added to the resin and the mixture shaken gently for 1.5 h. The resin was filtered and washed with TFE/DCM (1:4, 6 mL). The purple filtrate was collected and the solvent was evaporated under reduced pressure to provide a dark purple solid (0.205 g, 87%). C₄₂H₅₀Cl₃N₁₁Na₂O₁₀PtS (1248.41): calcd. C 40.41, H 4.04, N 12.34; found C 40.36, H 4.06, N 12.09.

X-ray Crystal Structure Determination: The crystallographic data and associated collection parameters for this complex are summarised in Table 5. CCDC-698463 contains the supplementary crystallographic data for this paper. These data can be obtained free of charge from The Cambridge Crystallographic Data Centre via www.ccdc.cam.ac.uk/data_request/cif.

Table 5. Crystallographic data and associated collection parameters for the species [Pt(terpy)(mpa)]⁺.

Empirical formula	C ₃₆ H ₃₂ AgCl ₂ N ₆ O ₉ Pt ₂ S ₂
Molecular weight	1325.77
Crystal system	triclinic
Space group	<i>P</i> 1̄ (No. 2)
<i>a</i>	10.1504 (1) Å
<i>b</i>	11.0400 (1) Å
<i>c</i>	20.0658 (2) Å
<i>V</i>	2194.9(4) Å ³
<i>α</i>	80.0575(4)°
<i>β</i>	89.4286(4)°
<i>γ</i>	82.3498(4)°
<i>D</i> _c	2.01 g/cm ³
<i>Z</i>	2
Crystal size	0.40 × 0.10 × 0.02 mm
Absorption coefficient	7.073 mm ⁻¹
<i>F</i> (000)	1262
Crystal colour	red
Crystal habit	plate
<i>λ</i> (Mo- <i>K</i> _α)	0.71073 Å
Transm.(Gaussian) _{min.,max.}	0.35, 0.87
<i>θ</i> range for data collection	5–27°
<i>2θ</i> _{max}	55°
<i>hkl</i> range	–13 ≤ <i>h</i> ≤ 13, –14 ≤ <i>k</i> ≤ 14, –26 ≤ <i>l</i> ≤ 26
<i>N</i>	18041
<i>N</i> _{ind}	13874
<i>N</i> _{obs}	13874
<i>N</i> _{var}	498
Completeness to <i>θ</i>	26.953 (99.2%)
Final <i>R</i> indices [<i>I</i> > 3σ(<i>I</i>)]	<i>R</i> ₁ (<i>F</i>) = 0.0386, <i>wR</i> (<i>F</i>) = 0.0476
Goodness-of-fit on <i>F</i> ²	1.0365

Supporting Information (see footnote on the first page of this article): Details of the synthesis and characterisation of chloroterpyridineplatinum(II) chloride and 4-[(9-fluorenylmethoxycarbonyl)amino]-*N*-methylpyrrole-2-carboxylic acid.

Acknowledgments

The authors would like to thank the University of Western Sydney for the financial support through internal research grants and PhD scholarships. M. v. H. would like to thank the University of Western Sydney – College of Health Sciences for generous support through a writing fellowship.

- [1] J. Hartman, H. Lipp, *Expert Opin. Pharmacother.* **2003**, *4*, 889–901.
- [2] O. Rixe, W. Ortuzar, M. Alvarez, R. Parker, E. Reed, K. Paull, T. Fojo, *Biochem. Pharmacol.* **1996**, *52*, 1855–1865.
- [3] J. Misset, H. Bleiberg, W. Sutherland, M. Bekradda, E. Cvitkovic, *Crit. Rev. Oncol. Hematol.* **2000**, *35*, 75–93.
- [4] H. E. Moser, P. B. Dervan, *Science* **1987**, *238*, 645–650.
- [5] M. Isomura, H. Sugiyama, I. Saito, *Nucleic Acids Symp. Ser.* **1995**, *34*, 47–48.
- [6] H. Sugiyama, C. Lian, M. Isomura, I. Saito, A. H. Wang, *Proc. Natl. Acad. Sci. USA* **1996**, *93*, 14405–14410.
- [7] Z. Tao, T. Fujiwara, I. Saito, H. Sugiyama, *Am. Chem. Soc.* **1999**, *121*, 4961–4967.
- [8] T. Bando, A. Narita, I. Saito, H. Sugiyama, *Chem. Eur. J.* **2002**, *8*, 4781–4790.
- [9] N. L. Fregeau, Y. Wang, R. T. Pon, W. A. Wylie, J. W. Lown, *J. Am. Chem. Soc.* **1995**, *117*, 8917–8925.
- [10] P. G. Baraldi, B. Cacciari, R. Romagnoli, G. Spalluto, R. Gambari, N. Bianchi, M. Passadore, P. Ambrosino, N. Mong-

- elli, P. Cozzi, C. Geroni, *Anti-Cancer Drug Des.* **1997**, *12*, 555–576.
- [11] Y. Wang, J. Dziegielewski, A. Y. Chang, P. B. Dervan, T. A. Beerman, *J. Biol. Chem.* **2002**, *277*, 42431–42437.
- [12] P. Mitra, R. L. Xie, R. Medina, H. Hovhannisyan, S. K. Zaidi, Y. Wei, J. W. Harper, J. L. Stein, A. J. van Wijnen, G. S. Stein, *Mol. Cell Biol.* **2003**, *23*, 8110–8123.
- [13] A. C. Finlay, F. A. Hochstein, B. A. Sobin, F. X. Murphy, *J. Am. Chem. Soc.* **1951**, *73*, 341–343.
- [14] A. Di Marco, M. Gaetani, P. Orezzi, F. Arcamone, *Cancer Chemother. Rep.* **1962**, *18*, 15–19.
- [15] M. L. Kopka, C. Yoon, D. S. Goodsell, P. Pjura, R. E. Dickerson, *Proc. Natl. Acad. Sci. USA* **1985**, *82*, 1376–1380.
- [16] X. Chen, B. Ramakrishnan, S. T. Rao, M. Sundaralingam, *Nat. Struct. Biol.* **1994**, *1*, 169–175.
- [17] K. Uytterhoeven, J. Sponer, L. van Meervelt, *Eur. J. Biochem.* **2002**, *269*, 2868–2877.
- [18] P. B. Dervan, *Bioorg. Med. Chem.* **2001**, *9*, 2215–2235.
- [19] D. S. Pilch, N. Poklar, C. A. Gelfand, S. M. Law, K. J. Breslauer, E. E. Baird, P. B. Dervan, *Proc. Natl. Acad. Sci. USA* **1996**, *93*, 8306–8311.
- [20] M. L. Kopka, D. S. Goodsell, G. W. Han, T. K. Chiu, J. W. Lown, R. E. Dickerson, *Structure* **1997**, *5*, 1033–1046.
- [21] N. C. Seeman, J. M. Rosenberg, A. Rich, *Proc. Natl. Acad. Sci. USA* **1976**, *73*, 804–808.
- [22] J. M. Wong, E. Bateman, *Nucleic Acids Res.* **1994**, *22*, 1890–1896.
- [23] C. L. Kielkopf, R. E. Bremer, S. White, J. W. Szewczyk, J. M. Turner, E. E. Baird, P. B. Dervan, D. C. Rees, *J. Mol. Biol.* **2000**, *295*, 557–567.
- [24] H. Loskotova, V. Brabec, *Eur. J. Biochem.* **1999**, *266*, 392–402.
- [25] H. Kostrhunova, V. Brabec, *Biochemistry* **2000**, *39*, 12639–12649.
- [26] D. Jaramillo, N. J. Wheate, S. F. Ralph, W. A. Howard, Y. Tor, J. R. Aldrich-Wright, *Inorg. Chem.* **2006**, *45*, 6004–6013.
- [27] R. I. Taleb, D. Jaramillo, N. J. Wheate, J. R. Aldrich-Wright, *Chem. Eur. J.* **2007**, *13*, 3177–3186.
- [28] J. X. McDermott, J. F. White, G. M. Whitesides, *J. Am. Chem. Soc.* **1976**, *98*, 6522–6528.
- [29] G. Annibale, M. Brandolisio, B. Pitteri, *Polyhedron* **1995**, *14*, 451–453.
- [30] K. W. Jennette, J. T. Gill, J. A. Sadownick, S. J. Lippard, *J. Am. Chem. Soc.* **1976**, *98*, 6159–6168.
- [31] B.-C. Tzeng, W.-F. Fu, C.-M. Che, H.-Y. Chao, K.-K. Cheung, S.-M. Peng, *J. Chem. Soc., Dalton Trans.* **1999**, 1017–1023.
- [32] S. A. Ross, G. Lowe, D. J. Watkin, *Acta Crystallogr., Sect. C* **2001**, *57*, 275–276.
- [33] G. Lowe, S. A. Ross, M. Probert, A. Cowley, *Chem. Commun.* **2001**, 1288–1289.
- [34] N. R. Wurtz, J. M. Turner, E. E. Baird, P. B. Dervan, *Org. Lett.* **2001**, *3*, 1201–1203.
- [35] E. Nishiwaki, S. Tanaka, H. Lee, M. Shibuya, *Heterocycles* **1988**, *27*, 1945–1952.
- [36] C. M. A. Hotzel, U. Pindur, *Eur. J. Med. Chem.* **2002**, *38*, 189–197.

Received: July 24, 2008

Published Online: September 3, 2008